Structural Basis for Antiarrhythmic Drug Interactions with the Human Cardiac Sodium Channel

Phuong T. Nguyen[1,3], Kevin R. DeMarco[1,3], Igor Vorobyov[1,2], Colleen E. Clancy[1,2], Vladimir Yarov-Yarovoy[1]

[1]Department of Physiology and Membrane Biology, University of California Davis, Davis, United States;
[2]Department of Pharmacology, University of California Davis, Davis, United States;
[3]Biophysics Graduate Group, University of California Davis, Davis, United States

ABSTRACT

The human voltage-gated sodium channel, hNaV1.5, is responsible for the rapid upstroke of the cardiac action potential and is target for antiarrhythmic therapy. Despite the clinical relevance of hNaV1.5 targeting drugs, structure-based molecular mechanisms of promising or problematic drugs have not been investigated at atomic scale to inform drug design. Here, we used Rosetta structural modeling and docking as well as molecular dynamics simulations to study the interactions of antiarrhythmic and local anesthetic drugs with hNav1.5. These calculations revealed several key drug binding sites formed within the pore lumen that can simultaneously accommodate up to two drug molecules. Molecular dynamics simulations identified a hydrophilic access pathway through the intracellular gate and a hydrophobic access pathway through a fenestration between domains III and IV. Our results advance the understanding of molecular mechanisms of antiarrhythmic and local anesthetic drug interactions with hNaV1.5 and will be useful for rational design of novel therapeutics.

METHODS

Detailed description of the methods is published in Nguyen PT et al. paper (1).

Rosetta modeling of the hNaV1.5 channel. We used the Rosetta structural modeling software (2) and the cryoEM structure of the NaV1.4-beta1 complex from the electric eel (eeNaV1.4) (PDB ID: 5XSY) (3) as a template to predict the structure of the human NaV1.5 (hNaV1.5) channel. 5,000 models of hNaV1.5 were generated and the top 500 lowest-scoring models were selected for clustering analysis. Models from top clusters were visually inspected to select the final model for the docking study.

RosettaLigand modeling of hNaV1.5 channel interaction with antiarrhythmic and local anesthetic drugs. Molecular docking of antiarrhythmic and local anesthetic drugs to hNaV1.5 channel model was performed using RosettaLigand (2). OpenEye OMEGA (OpenEye Scientific Software) (4) was used to generate conformers for each drug. To uniformly and efficiently sample the pore region of hNaV1.5, drugs were placed at 5 different initial locations: at the center of the cavity and at 4 fenestration sites. Sampling radius was set to 10 Å. A total of 200,000 docking models were generated for each drug. The top 10,000 models were selected based on the total score of protein-ligand complex and then ranked by ligand binding energy represented by Rosetta interface delta_X energy term.

Drug-membrane partitioning. Partitioning of charged and neutral lidocaine into a lipid membrane was assessed using the NAMD (5) program. Initial system setup scripts were generated with the CHARMM-GUI web toolkit (6) and were modified to build the hydrated drug-membrane systems, which consisted of 128 1-palmitoyl-2-oleoylphosphatidylcholine (POPC) lipids, ~7000 water molecules, 21 or 22 K+ and 22 Cl– ions to ensure 0.15 M electrolyte concentration and overall electrical neutrality, and one drug molecule, totaling ~38,250 atoms.

Molecular dynamics simulations of hNaV1.5 channel interaction with lidocaine. The hNaV1.5 model was embedded in a bilayer of POPC with explicit TIP3P water molecules and 150 mM (with lidocaine) or 500 mM (without lidocaine) of NaCl using CHARMM-GUI (7). For lidocaine containing simulations we used physiological NaCl concentration, but we used larger salt concentration in the drug-free runs to facilitate Na+ conductance. For all these simulations, we also used CHARMM36 lipid (8) and protein (9) force fields, and CHARMM generalized force field (CGENFF) compatible parameters.

ACKNOWLEDGMENTS

We would like to thank Drs. Jon Sack, Toby Allen, Heike Wulff, Kazuharu Furutani, Jie Zheng, and members of Clancy, Yarov-Yarovoy and Sack laboratories for helpful discussions. We thank Dr. Nieng Yan (Princeton University) for sharing coordinates of electric eel and human NaV1.4 channel structures. Anton 2 computer time was provided by the Pittsburgh Supercomputing Center (PSC) through Grant R01GM116961 from the National Institutes of Health. The Anton 2 machine (74) at PSC was generously made available by D.E. Shaw Research. This research was supported by National Heart, Lung, and Blood Institute Grant U01HL126273, R01HL128537, R01HL128170, OT2OD026580 to CEC and American Heart Association Predoctoral Fellowship 16PRE27260295 to KRD.

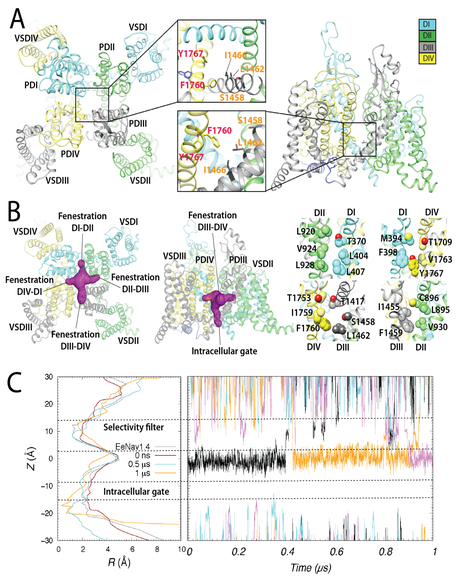

Fig. 1. Rosetta model of the hNav1.5 channel. (A) Extracellular (left panel) and transmembrane (right panel) views of the hNav1.5 model shown in ribbon representation. Insets – zoom-in views of putative drug binding residues within hNav1.5 pore lumen. Each domain is colored individually and labeled. In the insets, DIII residues are labeled orange, whereas DIV residues are labelled red. (B) Extracellular (left) and transmembrane (center and right) views of all four hNav1.5 fenestrations using molecular surface representation (shown in purple in the left and center panels). In the right panels, fenestration-facing residue side chains are labelled and shown in space-filling representations using corresponding domain colors, with O atoms shown in red. (C) Left panel, hNav1.5 pore lumen radius (R) profile changes during molecular dynamic simulation at time zero (colored red), at 0.5 μs (colored cyan), and at 1 μs (colored orange). A pore lumen R profile for a cryoEM eeNaV1.4 structure is also shown in gray for comparison. Right panel, Sodium ion trajectories within the pore-forming domain during a 1 □s molecular dynamic simulation of hNav1.5.

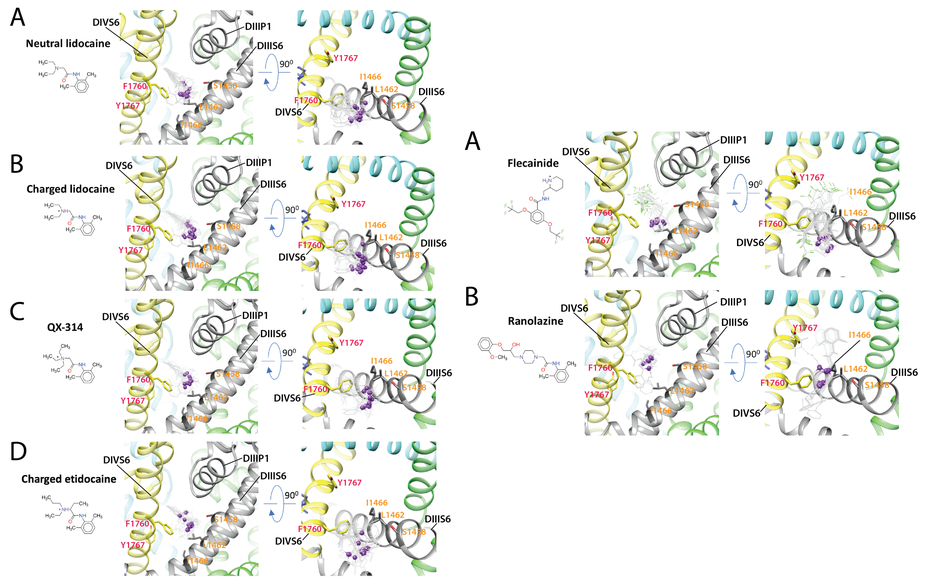

Fig. 2. Rosetta models of hNav1.5 channel interaction with antiarrhythmic and local anesthetic drugs. Close up transmembrane (left panels) and extracellular (right panels) views of hNav1.5 interactions with: (A) neutral lidocaine; (B) charged lidocaine; (C) QX-314; (D) charged etidocaine. Drug molecules are shown in the wireframe representations with basic N atoms depicted as purple balls. hNav1.5 domain I is colored in blue, domain II is colored in green, domain III is colored in gray, domain IV is colored in yellow. Side chains of key residues forming the receptor site in DIIIS6 and DIVS6 segments are shown in stick representation and labeled in orange and red, respectively.

Fig. 3. Rosetta models of hNav1.5 channel interaction with antiarrhythmic and local anesthetic drugs. Close up transmembrane (left panel) and extracellular (right panel) view of hNav1.5 interactions with (A) flecainide; (B) ranolazine. Drug molecules are shown in the wireframe representations with flecainide F atoms colored in green and basic N atoms of both drugs depicted as purple balls. hNaV1.5 domain I is colored in blue, domain II is colored in green, domain III is colored in gray, domain IV is colored in yellow. Side chains of key residues forming the receptor site in DIIIS6 and DIVS6 are shown in stick representation and labeled in orange and red, respectively.

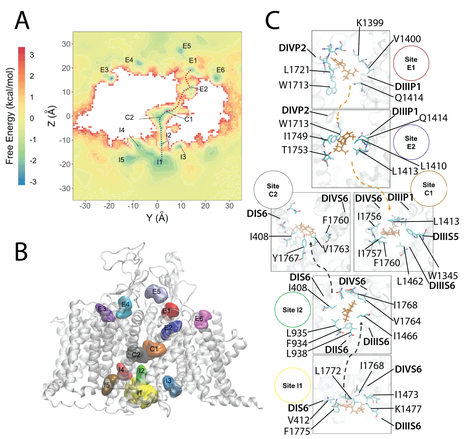

Fig. 4. Molecular dynamics simulation of the hNav1.5 channel interaction with neutral lidocaine reveals two drug access pathways. (A) Free energy surface of neutral lidocaine binding projected on the Y-Z plane (with Z corresponding to a transmembrane axis). Binding sites for neutral lidocaine, identified from free energy minima, are labeled as intracellular I1-5, channel pore C1-2, and extracellular E1-6. (B) Transmembrane view of the channel with neutral lidocaine binding sites represented as colored surfaces. Colors and sizes are for clarity, not actual binding properties. (C) Close-up view of binding sites forming the hydrophobic (orange arrows) and hydrophilic (gray arrows) binding pathways. Lidocaine molecules (orange) and interacting residues on the channel (cyan for C, red for O and blue for N) are shown using stick representation.

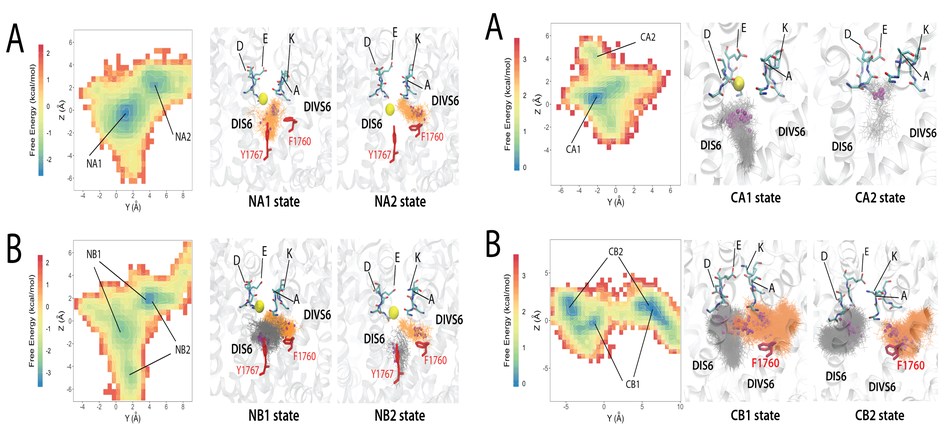

Fig. 5. Molecular dynamics simulation of the hNav1.5 channel interaction with neutral lidocaine reveal two binding poses: (A) states NA1 and NA2 for one lidocaine bound in the pore lumen; (B) NB1 and NB2 for two lidocaine molecules binding in the pore lumen at the same time. Left panels show free energy surfaces projected on the yz plane with binding sites identified from free energy minima and labeled. Middle and right panels show close-up transmembrane views of molecular models of charged lidocaine binding. In the close-up views lidocaine molecules (orange and dark-gray) and interacting residues on the channel (red) as well as SF "DEKA" motif (cyan for C, blue for N and red for O) are shown using stick representation. Lidocaine basic N atoms are shown as small purple spheres, and a SF bound Na+ atom is shown as yellow sphere.

Fig. 6. Molecular dynamics simulation of hNav1.5 channel interaction with charged lidocaine reveal two binding poses: (A) states CA1 and CA2 for one lidocaine bound in the pore lumen; (B) CB1 and CB2 for two lidocaine molecules binding in the pore lumen at the same time Left panel shows free energy surface projected on the yz plane with binding sites identified from free energy minima and labeled. Middle and right panels show close-up transmembrane views of molecular models of charged lidocaine binding. Selectivity filter "DEKA" motif residues are shown in stick representation and colored in cyan for C, blue for N and red for O. Sodium ions are shown as spheres and colored in yellow. Lidocaine molecules are shown in stick representation and colored in gray or orange. The nitrogen atoms of the tertiary ammonium groups on charged lidocaine molecules are shown as small spheres and colored in purple. The F1760 sidechain is shown in stick representation and colored in red.

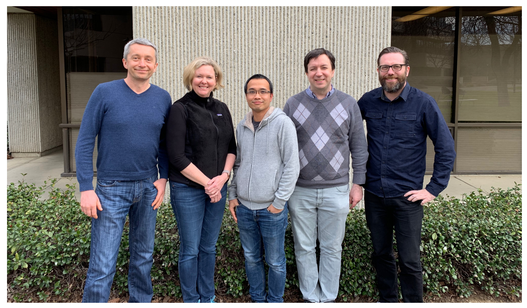

Left to right: Vladimir Yarov-Yarovoy, Colleen Clancy, Phuong Tran Nguyen, Igor Vorobyov and Kevin DeMarco

CONCLUSIONS

Our structural modeling and simulation of antiarrhythmic and local anesthetic drugs interaction with the human Nav1.5 channel revealed the following key observations:

1. Our hNav1.5 model does not conduct sodium ions under applied voltage, which suggests that it does not represent an open conductive state (Fig. 1C);
2. The region above F1760 in the DIVS6 segment forms a "hot spot" for drug binding and extends from the fenestration region between the DIIIS6 and DIVS6 segments to the hydrophobic pockets under the selectivity filter regions in DIII and DIV, which agrees with experimental data that identified key residues forming the high affinity drug binding to NaV channels in an inactivated state (Figs. 2, 3, 5, and 6);
3. The amine/ammonium group of lidocaine, etidocaine, and QX-314 is positioned above and near F1760 (Fig. 2). The phenyl ring of lidocaine, etidocaine, and QX-314 is observed in multiple different orientations near F1760 (Fig. 2);
4. Flecainide and ranolazine bind to a larger protein surface area that spans from the fenestration region between the DIII and DIV to the ion conduction pathway under the selectivity filter region (Fig. 3);
5. Lidocaine enters the hNav1.5 pore via the hydrophilic pathway through the intracellular gate and via a novel hydrophobic pathway through the vertical lipid – channel interface formed by the P1-helix in DIII, P2-helix in DIV, and DIII-DIV fenestration (Fig. 4 and Supplemental Movie 2);
6. Up to two lidocaine molecules can simultaneously bind within the hNav1.5 pore lumen, which agrees with experimental data demonstrating cooperative binding of multiple lidocaine molecules to Nav channels in an inactivated state (80) (Figs. 5 and 6);
7. Bound lidocaine molecules can interfere with the ion occupancy in the hNav1.5 SF. Based on our results, we suggest that our hNav1.5 model is consistent with an inactivated state.

REFERENCES

1. Nguyen PT, DeMarco KR, Vorobyov I, Clancy CE, & Yarov-Yarovoy V (2019) Structural basis for antiarrhythmic drug interactions with the human cardiac sodium channel. Proc Natl Acad Sci U S A 116(8):2945-2954.

2. Bender BJ, et al. (2016) Protocols for Molecular Modeling with Rosetta3 and RosettaScripts. Biochemistry 55(34):4748-4763.

3. Yan Z, et al. (2017) Structure of the Nav1.4-beta1 Complex from Electric Eel. Cell 170(3):470-482 e411.

4. Hawkins PC & Nicholls A (2012) Conformer generation with OMEGA: learning from the data set and the analysis of failures. J Chem Inf Model 52(11):2919-2936.

5. Phillips JC, et al. (2005) Scalable molecular dynamics with NAMD. Journal of Computational Chemistry 26(16):1781-1802.

6. Jo S, Kim T, Iyer VG, & Im W (2008) CHARMM-GUI: A web-based graphical user interface for CHARMM. Journal of Computational Chemistry 29(11):1859-1865.

7. Jo S, Kim T, Iyer VG, & Im W (2008) CHARMM-GUI: a web-based graphical user interface for CHARMM. J Comput Chem 29(11):1859-1865.

8. Lee S, et al. (2014) CHARMM36 united atom chain model for lipids and surfactants. J Phys Chem B 118(2):547-556.

9. Huang J & MacKerell AD, Jr. (2013) CHARMM36 all-atom additive protein force field: validation based on comparison to NMR data. J Comput Chem 34(25):2135-2145.